Carbon 95 (2015) 302–308

Contents lists available at ScienceDirect

Carbon

journal homepage: www.elsevier.com/locate/carbon

Differentiation of chemical reaction activity of various carbon nanotubes using redox potential: Classification by physical and chemical structures

Shuji Tsuruoka [a, *], Hidetoshi Matsumoto [b, **], Vincent Castranova [c], Dale W. Porter [d], Takashi Yanagisawa [e], Naoto Saito [f], Shinsuke Kobayashi [f], Morinobu Endo [g]

[a] Aquatic Innovation Center, Shinshu University, 4-17-1 Wakasato, Nagano 380-8553, Japan
[b] Department of Organic and Polymeric Materials, Tokyo Institute of Technology, 2-12-1 Ookayama, Meguro-ku, Tokyo 152-8552, Japan
[c] West Virginia University, Morgantown, WV, USA
[d] Pathology & Physiology Research Branch, National Institute for Occupational Safety and Health, 1095 Willowdale Rd. (M/S2015), Morgantown, WV, USA
[e] GSI Creos Corporation, 1-12, Minami-Watarida-cho, Kawasaki, Kanagawa 210-0855, Japan
[f] Department of Applied Physical Therapy, Shinshu University, School of Health Sciences, 3-1-1 Asahi, Matsumoto, Nagano, Japan
[g] Institute of Carbon Science and Technology, Shinshu University, Nagano 380-8553, Japan

ARTICLE INFO

Article history:
Received 7 April 2015
Received in revised form
4 July 2015
Accepted 15 August 2015
Available online 17 August 2015

ABSTRACT

The present study systematically examined the kinetics of a hydroxyl radical scavenging reaction of various carbon nanotubes (CNTs) including double-walled and multi-walled carbon nanotubes (DWCNTs and MWCNTs), and carbon nano peapods ($AuCl_3$@DWCNT). The theoretical model that we recently proposed based on the redox potential of CNTs was used to analyze the experimental results. The reaction kinetics for DWCNTs and thin MWCNTs agreed well with the theoretical model and was consistent with each other. On the other hand, thin and thick MWCNTs behaved differently, which was consistent with the theory. Additionally, surface morphology of CNTs substantially influenced the reaction kinetics, while the doped particles in the center hollow parts of CNTs ($AuCl_3$@DWCNT) shifted the redox potential in a different direction. These findings make it possible to predict the chemical and biological reactivity of CNTs based on the structural and chemical nature and their influence on the redox potential.

1. Introduction

Carbon nanotubes (CNTs) have been predicted useful for various medical, commercial and industrial applications, and designing their structures has recently become an important issue in order to obtain tailor-made performances [1,2]. Industrially, modifications of CNT structures have become an important issue to obtain appropriate functionalities and safety in use, because multi-walled CNTs (MWCNTs) are applied and commercialized broadly. Under the circumstance a crucial goal will be to design safe CNT structures, since toxicological evaluations on CNTs are advancing leading to a predictive exposure limit for MWCNTs [3]. Our previous article [4] clarifies that the surface chemical reactivity of MWCNTs agrees with the redox potential hypothesis in light of the scavenging reaction of hydroxyl radicals, and discusses this groundbreaking challenge that requires identification of a key control mechanism of toxicological phenomena. The relative importance of specific physicochemical properties has not been defined explicitly, while critical points concerning CNT safety evaluations are summarized as the fiber paradigm and bioactivity, *e.g.*, metal impurities of CNTs [5]. The former refers to effects of physical contact with cells and tissues. The latter refers to chemical reactions on the CNT surface, relating to reaction kinetics of CNTs. In this regard, CNT chemical reactivity must be explored based on redox reactions. Although metallic impurities of CNTs have been discussed elsewhere [6–13], a reaction mechanism for CNTs is not beyond expectations [14–18]. Those researchers used hydroxyl radicals to explore the surface reactivity of CNTs because they were keen to determine whether reactive oxygen species were generated by CNTs. A recent report, concerning surface reactivity of single-walled nanotubes (SWCNTs) with oxidant species, discussed the redox potential kinetically [19].

* Corresponding author.
** Corresponding author.
E-mail addresses: Tsuruoka.saitama@gmail.com (S. Tsuruoka), matsumoto.h.ac.@m.titech.ac.jp (H. Matsumoto).

http://dx.doi.org/10.1016/j.carbon.2015.08.048
0008-6223/

Even though many researches strove to find out the reaction mechanism, the reactivity on carbon basal planes or graphene has been limited within solid-state functions.

A classic report concluded that active reaction sites of graphenes were at the edges [20]. After this report, chemical reactivity with various carbon surfaces was measured; the conversion rate of carbon to methane was a typical indicator [21]. On the other hand, the rate limiting process of carbon redox reaction was investigated using a conversion from Fe^{2+} to Fe^{3+} on carbon electrodes [22]. It is noteworthy that a popular method of voltammetry to determine chemical reactivity on a solid surface has limitations and is not generally applicable to measurement of true reactivity of particle material surfaces [23,24]. Nugent et al. reported that electron transfer rate can be specified on a carbon surface using a reaction of Fe^{2+} to Fe^{3+} in order to determine the redox potential [25]. However, they did not discuss affinity between Fe and carbon well, though it is known that Fe forms carbide with carbons at room temperature. Meanwhile, Menéndez et al. showed detailed reaction kinetics of graphene theoretically and experimentally [26]. The authors pointed out the importance of unpaired electrons at the carbons of a graphene basal plane. This supports Andrieux [22] and Nugent's [25] discussions, implying that functions of carboxyl moieties and oxygen atoms on CNT surfaces have not been understood appropriately. They concluded as quoted, "*main contribution to carbon surfaces is from oxygen-free Lewis* (acid and) *base sites with graphene layers*", where the reaction kinetics relates to redox potential. Radovic reported and strengthened the point by the mathematical study of the reactions [27]. In addition, the discussion was supported by CNTs' stabilization in reduction reactions of fuel cells [28]. Peng et al. found that MWCNTs doped with cadmium sulfide (CdS) were electron acceptors and catalyzed conversion of water to hydrogen (and inevitably oxygen) in a photoreaction, where radical formation and degeneration were implicitly included [29]. This shows that MWCNTs are both electron acceptors and donators in redox reactions depending on their relative chemical potentials. Those investigations suggest that CNTs behave as electron acceptors as a Lewis acid under a certain condition.

SWCNTs and DWCNTs are particularly unique because they form carbon nano "Peapods" without changing surface structure. Peapods can be utilized for the semiconductor materials of electronic devices (*e.g.*, field-effect transistors and sensors) [30] and the templates leading to the formation of supra-molecular and 1-D nanostructures [30,31]. Although there has been interestingly no report in which chemical reactivity is measured experimentally, the first principle calculations of reactivity have been conducted and reported [32–35]. These articles specified particular structures and/or reaction conditions to solve those first principle equations numerically, even though the boundary conditions are not realistic. Chemical reactions of peapods were physically investigated using fullerene@SWCNTs [36,37]; however, these authors merely predicted the possibilities of electron behaviors on peapod surfaces rather than reporting experimental results. It is of interest that all of those reports determined or pre-determined CNTs as p-type materials instead of adopting general acid-base understandings.

The present work objectively investigated chemical reactivity of the CNT surface. Firstly, the hypothesis on CNT redox potential established in our previous report [4] was applied to evaluations of different types of CNTs in order to prove its generalizability. CNTs with different diameter and surface morphology were chosen to pursue it. Secondly, a grouping of CNTs was attempted in terms of the physical properties and scavenging reaction behaviors. The established experimental method [4] was adopted, where hydroxyl radical scavenging was measured by the electron spin resonance (ESR) method. The present work presents a method to predict CNT redox potential using their physicochemical properties.

2. Experimental

2.1. CNTs and peapods

Fig. 1 shows TEM images of CNTs used in the present work, except Nanocyl N-7000, using JEM-2100 equipped with Cs-corrected unit EM-Z07167T, JOEL, Tokyo, Japan. The physical properties are summarized in Table 1 and can be found elsewhere [38,39]. DWCNTs were purchased from Toray Industries, Inc., Tokyo Japan. Surface modified MWCNTs were prepared from Creos 24PS (GSI Creos Corporation, Tokyo, Japan) and characterized by GSI Creos Corporation (Tokyo, Japan). The average diameter and length of Creos 24PS were 80 nm and 5 μm, respectively, and the detail characteristics of Creos 24PS were reported elsewhere [4]. Creos AR50 was mechanically milled on the surface of Creos 24PS. Creos AR50HT-Pt prepared was graphitized at 2800 °C in argon atmosphere and deposited platinum by 20 wt% on the surface. Creos Dew 60 was modified Creos 24PS surface that was exposed to nitric acid in order to dope oxygen atoms. O1s on the surface of Creos Dew 60 were about twice as much as that of Creos 24PS by X-ray photoelectron spectroscopy (XPS, Shimadzu AXIS Ultra, Kyoto, Japan) analysis. The average diameter and length of Nanocyl NC-7000 were 9.5 nm and 1.5 μm, respectively.

Peapods of $AuCl_3$@DWCNT were synthesized in our lab. The obtained Toray DWCNTs were washed in deionized pure water and ethanol to remove dispersant and residues, and then heated at 383 K to remove moisture. The peapods were synthesized using a glassware apparatus depicted in Fig. S1 in Supplemental. One hundred mg of DWCNTs were weighed on an electronic balance and placed in the main tube of a two-way Pyrex® glass tube. One hundred mg of $AuCl_3$ (Wako Pure Chemical Industries, Osaka, Japan) was placed in the side tube. The main tube was heated in a heating mantle at 423 K and de-gassed using a vacuum pump. This de-gassing was conducted in two steps; the DWCNTs were first dried and then a target pressure was achieved. After reaching 10^{-5} Pa inside the tube, the tube neck was melted and sealed. The main and side tubes were placed in a heating mantle at 773 K for 24 h, cooled down to room temperature, and peapods were taken out from the main tube. The synthesized peapods were washed in diluted HCl solution (1 mol/L) to remove excess $AuCl_3$ particles on the CNT surfaces, and then washed by excess distilled water and dried. The peapods were stored in a desiccator. Transmission electron microscopy and X-ray fluorescence (XRF, Rigaku XRF ZSX Primus II, Tokyo, Japan) analysis spectroscopy of those peapods are shown in Fig. 2. A simplified analysis that was installed in the XRF (Application Package, EZS103MNV) was conducted to determine the amount of Au in the peapods; the atomic concentration of $AuCl_3$ was approximately 3 mass% of the peapods.

Measurements of scavenging of hydroxyl radicals by CNTs were conducted using the ultra-low concentration surfactant method (Tsuruoka–Matsumoto method), where surfactant was controlled to a minimal concentration against MWCNT mass. By the method, the good dispersion of CNTs in water was obtained, and the influence of surfactant was minimized in the analysis. The method characteristically uses substrate, such as polyester fibers, on which the pre-dispersed CNTs are held and from which the CNTs with residual surfactant are dispersed homogeneously into pure water. CNTEC® was made of polyester fibers coated with 12 wt% Nanocyl NC-7000 in a dry condition. Weight ratio of concentration of the surfactant to MWCNTs of CNTEC® was specially fixed at 26.2–100 in a dry condition. CNTEC® fibers (0.1 g) were dispersed into 50 g of ultrapure water, which was sonicated for 30 min in an ultrasonic bath. The mixture was filtered through a Whatman filter paper (Whatman 42) to remove polyester fibers and large agglomerates of MWCNTs. The solution was filtered with a Whatman filter paper

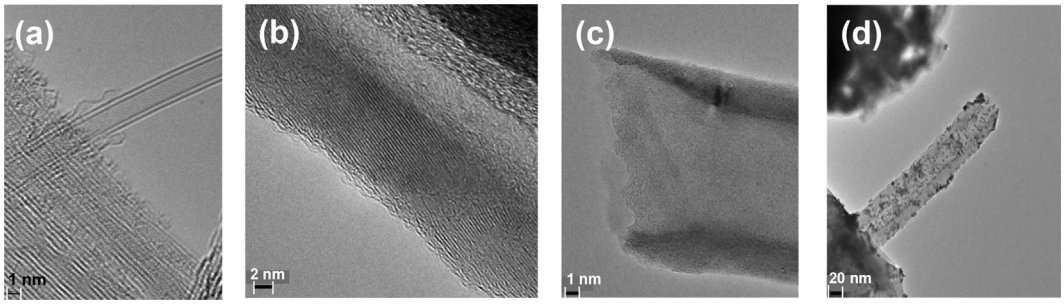

Fig. 1. TEM images of CNTs used in the present work. (a) Toray DWCNT, (b) Creos 24PS, (c) Creos AR50, (d) Creos AR50HT-Pt.

Table 1
CNT properties used in the present work.

	Ave. Diameter [nm]	Ave. Length [μm]	Purity [%]	Making methods	Note
DWCNT	<1.5	N/A	>95	CVD	As supplied
Nanocyl N-7000	10~15	~10	>90	CVD	As supplied
Creos 24 PS	80~100	5	>95	FCM*	Creos Basic
Creos AR50	80~100	5	>95	FCM*	24PS milled Mechanically
Creos Dew 60	80~100	5	>95	FCM*	24PS treated with Nitric Acid
Creos AR50HT-Pt	80~100	5	>95 as CNT	FCM*	AR50 heat-treated at 2800 °C and 20% Pt deposited

* FCM stands for floating catalyst method.

(GF/F) and then a Milipore filter (MF-Milipore GSWP 09000m). This filtered solution included 0.036 wt% of MWCNTs. The procedure gave the advantage of minimizing the surfactant interference despite MWCNT concentration alterations. In all measurement, peroxide concentration was in excess. The other CNTs were similarly dispersed into pure water from polyester fibers of CNTEC-mimics and surfactant concentration was around 1/10 of the CNT level. The individual content of CNTs in those CNTEC-mimics was as follows; Toray DWCNTs at 12.0 wt%, $AuCl_3$@DWCNT at 11.0 wt%, Creos 24PS at 12.1 wt%, Creos AR50 at 10.5wt%, Creos AR50HT-Pt at 9.2wt%, and Creos Dew 60 at 8.5wt%.

2.2. Preparation of mixtures measured and ESR-DMPO method

The measuring method was reported in our previous article [4]. The measuring mixture consisted of MWCNTs, hydrogen peroxide, ferrous chloride, and 5,5-dimethyl-1-pyrriline-1-oxide (DMPO). Hydrogen peroxide (hydrogen peroxide 30.0–35.5 mass%, Wako Pure Chemical Industries, Ltd. Japan) was diluted to 0.1 M with ultrapure water. The 0.1 M solution was diluted to 1 mM with ultrapure water and immediately consumed. Ferrous chloride (Iron (II) Chloride Tetrahydrate, Wako Pure Chemical Industries, Ltd., Osaka, Japan) was dissolved in ultrapure water to 15.7 mM. This solution was also diluted 100 times before use. Frozen DMPO (Dojindo Laboratories, Kumamoto Japan) was thawed at room temperature and diluted to 100 mM with ultrapure water. The mixture components are summarized in Table 2. Note that surfactant used in the present work was a zwitteronic type. The CNT solutions were prepared as mentioned above. The CNT concentrations in the solutions were measured by weighing CNTs after evaporation of those solutions.

2.3. Electron spin resonance measurement

All solutions were mixed and measured at room temperature with Electron Spin Resonance (ESR) (JES-FA100, JEOL). ESR settings were the same as the previous work [4]: frequency 9415.404 MHz, power 0.998 mW, field center 335 mT, sweep time 2 min, width ±5 mT, and modulation frequency 100 kHz. All measurements were conducted within 5 min after mixing all of those solutions.

ESR spectra were normalized using the mixture in Table 2 with 0.1 ml CNT solution for individual CNT measurements. Thus, the scavenge ratio represents the normalized hydroxyl radical concentration in a solution. All of the samples were assessed at least five times, and results were arithmetically averaged except the lowest and highest values. In the present work, pH buffer was not added because the buffer apparently affects the scavenging and adduct reactions. pH was not measured during ESR-DMPO measurement because a pH cell cannot be physically placed into the ESR cell.

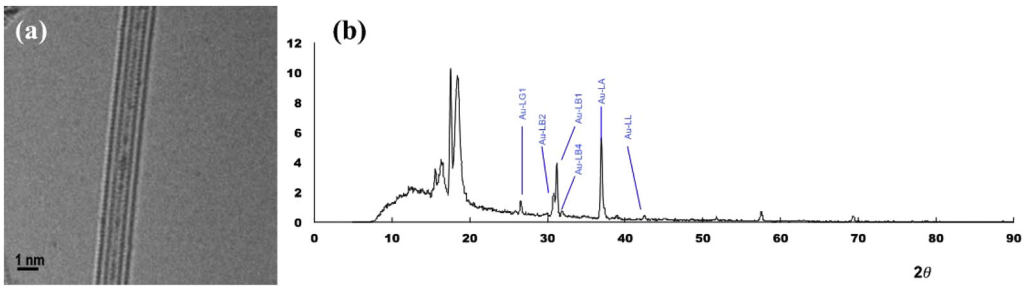

Fig. 2. (a) TEM image and (b) XRF spectrum of $AuCl_3$@DWCNT. The vertical axis unit of (b) is A.U. (A colour version of this figure can be viewed online.)

Table 2
Mixture components for CNT dispersion solutions.

Amount of solutions taken [ml]							
Solutions	$FeCl_2$	CNTs in surfactant	DMPO	Surfactant	H_2O_2	Ultrapure water	Total volume
Blank reference	0.4	None	0.4	0.4–0.8	0.4	Balance	2.0
Mixture	0.4	0–0.4	0.4	Balance	0.4	0.4	2.0

3. Results and discussion

3.1. ESR-DMPO method

The current spin trapping method indirectly measures radical concentrations using a spin adduct that forms the stable amine-oxide radical and relatively-long-lived free radicals. The adduct gives a measurable hyperfine coupling constant of spin, and the concentration of free radical is obtained by analyzing area or peak height of the ESR signal spectrum [40]. Among various spin trapping compounds, 5,5-dimethyl-1-pyrroline-N-oxide (DMPO) is often used for chemical radical spin trapping because it dissolves into aqueous solution and captures radical molecules well, showing high selectivity [41]. Shvedova et al. [14] discussed the issue that ferrous irons associated with SWCNTs can cause the decomposition of hydrogen peroxide or alkoxyl radicals peroxide from lipid, since the unpurified SWCNTs used in that study contained up to 30% iron residue. Murray et al. [42] reported thereafter that the OH radical generation mostly resulted from the iron residue through the Fenton reaction. Furthermore, Porter et al. [43] demonstrated that purified MWCNTs scavenged OH radicals generated by the Fenton reaction and did not generate ROS in an acellular system. Therefore, the ESR-DMPO method is considered a reliable method to measure hydroxyl radicals in aqueous solutions.

3.2. Reaction kinetics of DWCNTs and their peapods

Our hypothesis was adopted to analyze and evaluate results in the present work. According to the articles [26,27], the hydroxyl radical–carbon reaction occurs at dangling bonds on CNT surfaces, donating electrons to the radicals. As mentioned above, Peng et al. [29] found that MWCNTs attached with cadmium sulfide (CdS) were electron acceptors, but donated electrons to the other species simultaneously. This obviously shows that MWCNTs can be both electron acceptors and donators in redox reactions, depending on their relative chemical potentials. Using the Tsuruoka–Mtsumoto method [4], a simple system consisting of hydrogen peroxide and Fe (II) can be comprehensively written to characterize the reactions as;

$$3H_2O_2 \rightarrow 2H_2O + O_2 + 2HO\bullet \quad (1)$$

Since hydroxyl radicals can be scavenged in the CNT aqueous solution, assumed reaction sites on CNT surface (Dn) should be satisfied by the following equation:

$$2Dn + 2HO\bullet \rightarrow 2Dn^+ + H_2 + O_2 \quad (2)$$

Accordingly, Eq. (1) plus (2) give

$$3H_2O_2 + 2Dn \rightarrow 2Dn^+ + 2H_2O + H_2 + 2O_2 \quad (3)$$

Eq. (3) can be verified by concentration measurement of hydrogen and oxygen. However, it is experimentally impossible to do so in situ because the ESR equipment and measuring cell structure prohibits doing it physically. To avoid such experimental difficulty, Eq. (3) is solved in line with the reaction kinetics, and becomes;

$$S_{rad} = -q \ln|C_{Dn}| + qC_{Dn} + r \quad (4)$$

Or,

$$S_{rad} = -q \ln|C_{Dn} + s| + q(C_{Dn} + s) + r \quad (5)$$

where S_{rad} and C_{Dn}, are scavenging ratio and CNT concentration in a mixture, *and* q, r, and s are arbitrary constants. The detail derivation of those equations can be found in our previous article and its Supplemental material [4]. The CNT concentration is denoted by C_{Dn} and the arbitrary constant s is added to avoid taking C_{Dn} at zero in logarithmic axis numerically. Since characteristics for nanomaterials depend on their size and/or surface morphology, Eq. (5) has to include the nature of size. Therefore, the size is included among those arbitrary constants, C_{Dn} and s of the kinetically derived equation. And if so, when a set of those constants for a type of CNTs agrees with that of the other type of CNTs in Eq. (5), those two types of CNTs are regarded as having the identical kinetics. Originally those constants are determined by CNT concentration and reaction time, but they should eventually include an odd property such as size and surface morphology. To symbolize the point, a notion of "a nano-basis of CNTs" is introduced as a new concept to explain nanomaterial kinetics using Eq. (5).

Relationships between concentration ratio of hydroxyl radicals and CNT concentration are plotted in Fig. 3 using Toray DWCNTs, their peapods, and Nanocyl N-7000. Note that the result of Nanocyl N-7000 is from our previous article [4]. The experimental results and curve fitting using Eq. (5) are derived from Figs. S2–S5; the standard deviations are also presented in the figures. The calculated line for Toray DWCNTs obviously agrees with that of Nanocyl N-7000, and hence both sets of coefficients in Eq. (5) are almost identical. Since there exists an experimental limitation in which a CNT concentration cannot be easily controlled without agglomeration in an ultra low surfactant concentration, the ranges for both CNTs do not overlap completely. Despite of the condition Fig. 3 suggests that both of CNTs have the same kinetics. On the other hand, the peapods of $AuCl_3$@DWCNT do not agree with Toray DWCNTs at all, though they are postulated having the same surface

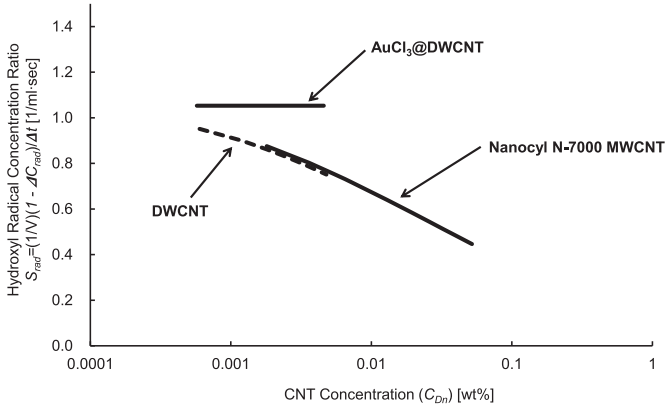

Fig. 3. Relationship between hydroxyl radical concentration ratio and CNT concentrations of Toray DWCNTs, $AuCl_3$@DWCNT peapods, and Nanocyl N-7000.

morphology and characteristics. In Fig. 3, as the peapod line lies around $S_{rad} = 1$ horizontally, the peapods are intrinsically inert in the scavenging reaction; electrons are not donated nor accepted on the peapod surface in the solution. The particles doped in the center hollow tubes significantly influenced the surface electron behaviors and redox reactions through the rolled graphene layers. The phenomena between Toray DWCNTs and Nanocyl MWCNTs were predicted [44], but had not been confirmed. In fact, the present work proves the point experimentally and the Eq. (5) is strengthen by the agreement with the prediction.

Surface reactivity of peapods has been measured and discussed based on work function in light of solid-state physics. Shiraishi and Ata measured work function values of HOPG, MWCNTs, and SWCNTs, and values were at 4.80, 4.95, and 5.05 eV, respectively [45]. The measurement was conducted using Ultraviolet Photoelectron Spectroscopy (UPS). In later studies, these values, using the same measurement method, were reported to range from 5.44 to 5.64 eV [46], and using thermionic emission method from 4.7 to 4.9 eV for SWCNTs, DWCNTs, and MWCMTs [47]. In those studies, CNTs were regarded as p-type semiconductors and electron acceptors. However, Kotimäki [48] conducted an elaborate experiment on the phenomena and pointed out that electron states of p- and n-types depended on electrode materials that were attached to CNTs. In addition, the electron states of CNT surfaces were significantly influenced by particles included in the center hollow tubes of SWCNTs. Note that Kotimäki used fullerenes and metallofullerenes as those particles instead of metals or metal oxides. From the study results, the author questioned a previous study [49] in which peapods including azafullerenes were determined as n-type. These discussions suggest that electrons on CNT surfaces are definitely affected by particles included in the inner hollow tubes of CNTs and the attached electrodes, and that work function of those surfaces depends on a measuring method and makeup. Also, since the values of work function for CNTs might be obtained in extreme and/or computable conditions, it is difficult to obtain the realistic chemical reactivity for CNTs in-situ, using work function.

The present work experimentally shows that electron behaviors on CNT surfaces are definitely influenced by particles included in the hollow tubes, and CNTs donate electrons to hydroxyl radicals. Although surface reactivity studies in the field of solid-state physics give CNTs p-type characteristics, the present results indicate that CNT surfaces can be electron donors in this particular condition. And the reactions can be characterized by chemical kinetics in Eq. (5), which suggests that chemical kinetics of CNT surface is determined by the coefficients of *q, r,* and *s*. They specify redox potential of CNTs and allow one to predict chemical reactivity of CNTs.

3.3. CNTs characterized by redox potential

Since there is a variety of physical sizes and surface morphologies of CNTs, it is necessary to investigate the similarity among these CNTs regarding the kinetics presented by Eq. (5). Fig. 4 shows a relationship between concentration ratio of hydroxyl radical and CNT concentrations with Nanocyl N-7000 and Creos 24PS. It is apparent that these sets of coefficients do not agree with each other, and a rapid decrease of S_{rad} for Creos 24PS with an increase of CNT concentration means significant contribution of the first term of the right-hand side of Eq. (5). The first term of C_{Dn} for Creos 24PS has a larger index than one because the line shows the rapid downward curve. The scavenging kinetics substantially differ from that of Toray DWCNTs or Nanocyl N-7000. A comparison between Figs. 3 and 4 shows there is a size-dependent threshold for the nano-basis of CNTs. From those experimental results, Creos 24PS must be segmented into a new discrete group of CNTs from Toray DWCNTs that have an identical kinetics to Nanocyl N-7000 in the scavenging reaction based on Eq. (5). On the other hand, as Creos 24PS has a large index of the concentration C_{Dn}, the kinetics are intrinsically different of that of the Toray or Nanocyl. Therefore, there exist two types among CNTs from the standing point of nano-basis.

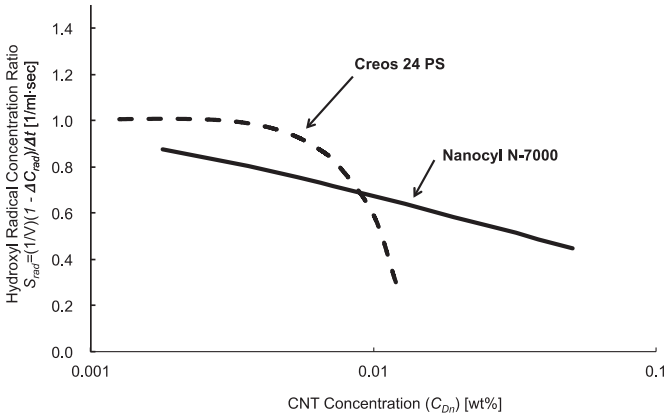

Fig. 4. Relationship between hydroxyl radical concentrations and CNT concentrations of Nanocyl N-7000 and Creos 24PS.

3.4. Nano-basis of CNTs with their morphology

Fig. 5 shows Creos 24PS and its derivatives. Surface morphologies of these derivatives were modified from Creos 24PS. Plots of experimental results with standard deviations are summarized in Fig. S5. All of the surface modified products interestingly have the similar reaction kinetics, even though they were individually modified and purposely had discrete surface morphologies. According to a previous article [26], hydroxyl radicals react with ketone or carboxyl on the CNT surfaces directly, so that the radicals might form C—H and/or C—O/C═O bonding on the Creos AR50 surface. Creos Dew 60, that was oxygen doped by nitric acid, might react with the radicals and the kinetic constant might be different from that of AR50. However, the enhanced scavenging reactions tend to be the catalytic reaction with platinum, though those tailings seem not to be the same. The present work cannot specify a reaction model among these derivatives. It should be considered a relationship between the reaction rate on those CNT surfaces and the Fenton reaction that is relatively slow [50,51].

As mentioned above, Toray DWCNTs and Nanocyl N-7000 have the identical nano-basis, and Creos 24PS can be segregated from

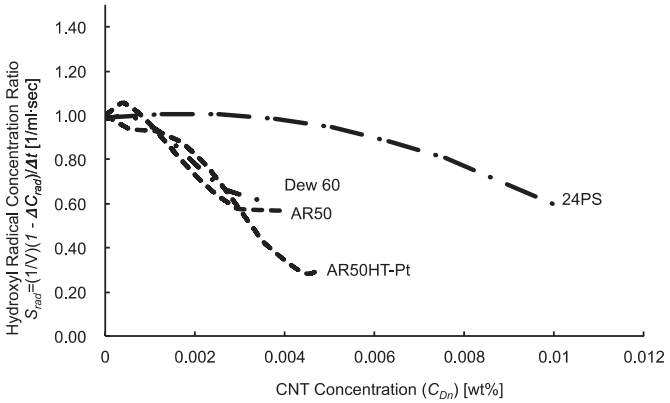

Fig. 5. Relationship between hydroxyl radical and CNT concentrations of Creos 24PS and its derivatives.

them in size. In Fig. 5, it should be considered that there exists another nano-basis distinguishing Creos 24PS from its derivatives in terms of surface morphology. Thus, in addition to the diameter size dependency of CNTs, these surface modifications can be grouped into another segment of the nano-basis classification. Even though those physical parameters are discrete, all of the segmentations can be analyzed by the kinetics expressed by Eq. (5). Although the segmentation of the nano-basis is based on the particular reaction system shown here, a mathematical expression of the Eq. (5) characterizes CNT reaction kinetics and predicts chemical reactivity, which allows one to postulate bioactivities without experimental results of *in-vivo* or *in-vitro* tests. In conclusion, Eq. (5) can be generally applied to redox reactions on the CNT surface. To generalize the redox potential of CNTs theoretically, it is necessary to further investigate the present experimental results with an assumption of electron pairs described by Menéndez et al. [26]. Such studies are beyond the scope of the present work.

4. Conclusion

The present study systematically examined the kinetics of hydroxyl radical scavenging reaction of various carbon nanotubes (CNTs), including double-walled and multi-walled carbon nanotubes (DWCNTs and MWCNTs) and carbon nano peapods ($AuCl_3$@DWCNT). The experimental results were analyzed using a theoretical model that we recently proposed based on the redox potential of CNTs. A hypothesis advocated in our previous article [4] was reproducibly verified by the present experimental results. The reaction kinetics for DWCNTs and thin MWCNTs act similarly according to the theoretical model. On the other hand, thin and thick MWCNTs behaved differently according to the theory. Additionally, surface morphology of CNTs substantially influences the reaction kinetics, while the doped particles in the center hollow parts of CNTs ($AuCl_3$@DWCNT) substantially depress scavenging potential. In conclusion, two types of nano-basis were found and discussed in the present work, one of thickness and another of surface morphology. These findings make it possible to predict the chemical and biological reactivity of CNTs based on the structural and chemical nature through the redox potential. Therefore, to implement the kinetic studies with CNTs, the Tsuruoka–Matsumoto method has been proved useful to conduct these measurements. This method contributes to understanding chemical kinetics of CNTs experimentally and suggests that CNTs can be both electron donors and acceptors, depending on reaction conditions.

Disclaimer

The findings and conclusions in this report are those of the authors and do not necessarily represent the views of the National Institute for Occupational Safety and Health.

Acknowledgments

S. Tsuruoka and H. Matsumoto are co-corresponding authors. This work is a part of the research program “Development of innovative methodology for safety assessment of industrial nanomaterials” supported by the Ministry of Economy, Trade and Industry (METI) of Japan. ST was supported by the Exotic Nanocarbon Project, Japan Regional Innovation Strategy Program by the Excellence, JST (Japan Science and Technology Agency). We would like to thank Mr. E. Akiba at Kuraray Living, Ltd., and Prof. B. Fugetsu at Hokkaido University for preparations of these CNTEC samples. Furthermore, we were pleased Mr. K. Koyama at Shinshu University contributed to the laboratory experiments.

Appendix A. Supplementary data

Supplementary data related to this article can be found at http://dx.doi.org/10.1016/j.carbon.2015.08.048.

References

[1] P. Eklund, P. Ajayan, R. Blackmon, A.J. Hart, J. Kong, B. Pradhan, A. Rao, A. Rinzler, WTEC Panel Report on International Assessment of Research and Development of Carbon Nanotube Manufacturing and Applications, World Technology Evaluation Center, Inc., Baltimore, MD, 2007.
[2] M. Endo, H. Muramatsu, T. Hayashi, Y.A. Kim, M. Terrones, M.S. Dresselhaus, Nanotechnology: ‘Buckypaper’ from coaxial nanotubes, Nature 433 (2005) 476.
[3] J. Howard, Current Intelligence Bulletin 65: Occupational Exposure to Carbon Nanotubes and Nanofibers, DHHS (NIOSH), 2013. Publication No. 2013-145.
[4] S. Tsuruoka, H. Matsumoto, K. Koyama, E. Akiba, T. Yanagisawa, F.R. Cassee, N. Saito, Y. Usui, S. Kobayashi, D.W. Porter, V. Castranova, M. Endo, Radical scavenging reaction kinetics with multiwalled carbon nanotubes, Carbon 83 (2015) 232–239.
[5] K. Donaldson, C.A. Poland, Nanotoxicity: challenging the myth of nano-specific toxicity, Curr. Opin. Biotechnol. 24 (2013) 724–734.
[6] L. Guo, D.G. Morris, X. Liu, C. Vaslet, R.H. Hurt, A.B. Kane, Iron bioavailability and redox activity in diverse carbon nanotube samples, Chem. Mater. 19 (2007) 3472–3478.
[7] C. Ge, F. Lao, W. Li, Y. Li, C. Chen, Y. Qiu, X. Mao, B. Li, Z. Chai, Y. Zhao, Quantitative analysis of metal impurities in carbon nanotubes: efficacy of different pretreatment protocols for ICPMS spectroscopy, Anal. Chem. 80 (2008) 9426–9434.
[8] M. Pumera, Carbon nanotubes contain residual metal catalyst nanoparticles even after washing with nitric acid at elevated temperature because these metal nanoparticles are sheathed by several graphene sheets, Langmuir 23 (2007) 6453–6458.
[9] M. Pumera, Y. Miyahara, What amount of metallic impurities in carbon nanotubes is small enough not to dominate their redox properties? Nanoscale 1 (2009) 260–265.
[10] C. Ge, Y. Li, J.-J. Yin, Y. Liu, L. Wang, Y. Zhao, C. Chen, The contributions of metal impurities and tube structure to the toxicity of carbon nanotube materials, NPG Asia Mater. 4 (2012) e32.
[11] R.J. Toh, A. Ambrosi, M. Pumera, Bioavailability of metallic impurities in carbon nanotubes is greatly enhanced by ultrasonication, Chem. Eur. J. 18 (2012) 11593–11596.
[12] Y. Liu, Y. Zhao, B. Sun, C. Chen, Understanding the toxicity of carbon nanotubes, Acc. Chem. Res. 46 (2013) 702–713.
[13] X. Liu, L. Guo, D. Morris, A.B. Kane, H. Hurt, Targeted removal of bioavailable metal as a detoxification strategy for carbon nanotubes, Carbon 46 (2008) 489–500.
[14] A.A. Shvedova, V. Castranova, E.R. Kisin, D. Schwegler-Berry, A.R. Murray, V.Z. Gandelsman, A. Maynard, P. Baron, Exposure to carbon nanotube material: assessment of nanotube cytotoxicity using human keratinocyte cells, J. Toxicol. Environ. Health A 66 (2003) 1909–1926.
[15] I. Fenoglio, M. Tomatis, D. Lison, J. Muller, A. Fonseca, J.B. Nagy, B. Fubini, Reactivity of carbon nanotubes: free radical generation or scavenging activity? Free Radic. Biol. Med. 40 (2006) 1227–1233.
[16] I. Fenoglio, G. Greco, M. Tomatis, J. Muller, E. Raymundo-Piñero, F. Béguin, A. Fonseca, J.B. Nagy, D. Lison, B. Fubini, Structural defects play a major role in the acute lung toxicity of multiwall carbon nanotubes: physicochemical aspects, Chem. Res. Toxicol. 21 (2008) 1690–1697.
[17] I. Fenoglio, E. Aldieri, E. Gazzano, F. Cesano, M. Colonna, D. Scarano, G. Mazzucco, A. Attanasio, Y. Yakoub, D. Lison, B. Fubini, Thickness of multiwalled carbon nanotubes affects their lung toxicity, Chem. Res. Toxicol. 25 (2012) 74–82.
[18] B. Fubini, I. Fenoglio, M. Tomatis, F. Turci, Effect of chemical composition and state of the surface on the tox- ic response to high aspect ratio nanomaterials, Nanomedicine 6 (2011) 899–920.
[19] Y. Liu, J. Liggio, S.-M. Li, D. Breznan, R. Vincent, E.M. Thomson, P. Kumarathasan, D. Das, J. Abbatt, M. Antiñolo, L. Russell, Chemical and toxicological evolution of carbon nanotubes during atmospherically relevant aging processes, Environ. Sci. Technol. (2015), http://dx.doi.org/10.1021/es505298d.
[20] N.R. Laine, F.J. Vastola, P.L. Walker Jr., The importance of active surface area in the carbon-oxygen reaction, J. Chem. Phys. 67 (10) (1963) 2030–2034.
[21] J.G. McCartry, H. Wise, Hydrogenation of surface carbon on alumina-supported nickel, J. Catal. 57 (1979) 406–416.
[22] C.P. Andrieux, J.M. Dumas-Bouchiat, J.M. Savéant, Catalysis of electrochemical reactions at redox polymer electrodes: kinetic model for stationary voltammetric techniques, J. Electroanal. Chem. 131 (1982) 1–35.
[23] P. Chen, R.L. McCreery, Control of electron transfer kinetics at glassy carbon electrodes by specific surface modification, Anal. Chem. 68 (1996) 3958–3965.
[24] B.Q. Wei, R. Vajtai, P.M. Ajayan, Reliability and current carrying capacity of carbon nanotubes, Appl. Phys. Lett. 79 (2001) 1172–1174.

[25] J.M. Nugent, K.S.V. Santhanam, A. Rubio, P.M. Ajayan, Fast electron transfer kinetics on multiwalled carbon nanotube microbundle electrodes, Nano Lett. 1 (2) (2001) 87–91.
[26] J.A. Menéndez, J. Phillips, B. Xia, L.R. Radovic, On the modification and characterization of chemical surface properties of activated carbon: in the search of carbons with stable basic properties, Langmuir 12 (1996) 4404–4410.
[27] L.R. Radovic, Active sites in graphene and the mechanism of CO_2 formation in carbon oxidation, J. Am. Chem. Soc. 131 (2009) 17166–17175.
[28] G. Girishkumar, K. Vinodgopal, P.V. Kamat, Carbon nanostructures on portable fuel cells: single-walled carbon nanotube electrodes for methanol oxidation and oxygen reduction, J. Phys. Chem. B 108 (2004) 19960–19966.
[29] T. Peng, P. Zeng, D. Ke, X. Liu, X. Zhang, Hydrothermal preparation of multi-walled carbon nanotubes (MWCNTs)/CdS nanocomposite and its efficient photocatalytic hydrogen production under visible light irradiation, Energy Fuels 25 (2011) 2203–2210.
[30] H. Shinohara, In pursuit of nanocarbons, Chem. Rec. 12 (2012) 296–305.
[31] H. Terrones, Beyond carbon nanopeapods, ChemPhysChem 13 (2012) 2273–2276.
[32] Y. Cho, S. Han, G. Kim, H. Lee, J. Ihm, Orbital hybridization and charge transfer in carbon nanopeapods, Phys. Rev. Lett. 90 (2003) 106402.
[33] A. Rochefort, Electronic and transport properties of carbon nanotube peapods, Phys. Rev. B 67 (2003) 115401.
[34] Y. Omata, Y. Yamagami, K. Tadano, T. Miyake, S. Saito, Nanotube nanoscience: a molecular-dynamics study, Phys. E 29 (2005) 454–468.
[35] S.W.D. Bailey, C.J. Lambert, The electronic transport properties of $N@C_{60}@(n, m)$ carbon nanotube peapods, Phys. E 40 (2007) 99–102.
[36] T. Pichler, C. Kramberger, P. Ayala, H. Shiozawa, M. Knupfer, M.H. Rümmeli, D. Batchelor, R. Kitaura, N. Imazu, K. Kobayashi, H. Shinohara, Bonding environment and electronic structure of Gd metallofullerene and Gd nanowire filled single-wall carbon nanotubes, Phys. Stat. Sol. b 245 (2008) 2038–2041.
[37] N.M. Alpatova, N.F. Gol'dshleger, E.V. Ovsyannikova, Electrochemistry of fullerenes immobilized on the electrodes, Russ. J. Electrochem. 44 (2008) 78–90.
[38] S. Kobayashi, S. Tsuruoka, U. Usui, H. Haniu, K. Aoki, S. Takanashi, M. Okamoto, H. Nomura, M. Tanaka, S. Aiso, M. Saito, H. Kato, N. Saito, An Advanced In-situ Imaging Method Using Heavy Metal Doped Hollow Tubes to Evaluate the Biokinetics of Carbon Nanotubes in Vivo, 2015 (in print).
[39] T. Fujimori, A. Morelos-Gómez, Z. Zhu, H. Muramatsu, R. Futamura, K. Urita, M. Terrones, T. Hayashi, M. Endo, S.Y. Hong, Y.C. Choi, D. Tománek, Kaneko, Conducting linear chains of sulphur inside carbon nanotubes, Nat. Commun. 4 (2013) 2162.
[40] J.R. Harbour, V. Chow, J.R. Bolton, An electron spin resonance study of the spin adducts of OH and HO_2 radicals with nitrones in the ultraviolet photolysis of aqueous hydrogen peroxide solutions, Can. J. Chem. 52 (1974) 3549–3553.
[41] M. Kohno, Dojin News 117 (2006). www.dojindo.co.jp/letterj/117/index.html.
[42] A.R. Murray, E. Kisin, S.S. Leonard, S.H. Young, C. Kommineni, V.E. Kagan, V. Castranova, A.A. Shvedova, Oxidative stress and inflammatory response in dermal toxicity of single-walled carbon nanotubes, Toxicology 257 (2009) 161–171.
[43] D.W. Porter, A.F. Hubbs, R.R. Mercer, N. Wu, M.G. Wolfarth, K. Sriram, S. Leonard, L. Battelli, D. Schwegler-Berry, S. Friend, M. Andrew, B.T. Chen, S. Tsuruoka, M. Endo, V. Castranova, Mouse pulmonary dose- and time course-responses induced by exposure to multi-walled carbon nanotubes, Toxicology 269 (2010) 136–147.
[44] S. Tsuruoka, K. Takeuchi, K. Koyama, T. Noguchi, M. Endo, F. Tristan, M. Terrones, N. Saito, Y. Usui, D.W. Porter, V. Castranova, ROS evaluation for a series of CNTs and their derivatives using an ESR method with DMPO, J. Phys. Conf. Ser. 429 (2013) 012.
[45] M. Shiraishi, M. Ata, Work function of carbon nanotubes, Carbon 39 (2001) 1913–1917.
[46] G. Zhuo, Y. Kawazoe, First-principles study on work function of carbon nanotubes, Phys. B 323 (2002) 196–198.
[47] P. Liu, Q. Sun, F. Zhu, K. Liu, K. Jiang, L. Liu, Q. Li, S. Fan, Measuring the work function of carbon nanotubes with thermionic method, Nano Lett. 8 (2) (2008) 647–651.
[48] V. Kotimäki, Carbon Nanotube Azafullerene Peapods and Their Electronic Transport Properties, Pro Gradu thesis, University of Jyväskylä, 2008, URN_NBN_fi_jyu-200811145877.pdf.
[49] T. Kaneko, Y. Li, S. Nishigaki, R. Hatakeyama, Azafullerene encapsulated single-walled carbon nanotubes with n-type electrical transport property, J. Am. Chem. Soc. 130 (2008) 2714–2715.
[50] Y. Takuma, Reaction Rate in Decomposition of Volatile Organic Compounds Using Fenton's Reaction. Bulletin of TIRI 3 (Ph.D. dissertation), Tokyo Institute of Technology, 2008, 11719520102.
[51] M.L. Kremer, Mechanism of the Fenton reaction. Evidence for a new intermediate, Phys. Chem. Chem. Phys. 1 (1999) 3595–3605.